

Near-field scanning optical microscopy using a super-resolution cover glass slip

Yu-Hsuan Lin^{1,2} and Din Ping Tsai^{1,3,4,*}

¹Instrument Technology Research Center, National Applied Research Laboratories, Hsinchu 30076, Taiwan

²Department of Electrophysics, National Chiao Tung University, Hsinchu 30010, Taiwan

³Department of Physics, National Taiwan University, Taipei 10617, Taiwan

⁴Research Center for Applied Sciences, Academia Sinica, Taipei 115, Taiwan

*dptsai@phys.ntu.edu.tw

Abstract: This study presents a novel near-field optics technology. A near-field cover glass slip (NF-CGS) was developed to improve the resolution of optical microscopy beyond the diffraction limit. A multi-layered structure of cover glass/ZnS-SiO₂ (130 nm)/AgO_x (15 nm)/ ZnS-SiO₂ (40 nm) was employed to generate the optical coupling effect for increasing the contrast and enhancing resolution of imaging. This novel innovation is expected to be employed in near-field imaging techniques for samples in different environments because of its simplicity, rapid laser scanning, and minimal costs. Experimental results of 500 nm, 200 nm, and 100 nm standard polystyrene nanospheres on NF-CGS and normal cover glass are demonstrated and imaged by using a laser scanning confocal microscope.

©2012 Optical Society of America

OCIS codes: (180.4243) Near-field microscopy; (240.6680) Surface plasmons.

References and links

1. E. A. Ash and G. Nicholls, "Super-resolution aperture scanning microscope," *Nature* **237**(5357), 510–512 (1972).
2. D. W. Pohl, W. Denk, and M. Lanz, "Optical stethoscopy: image recording with resolution $\lambda/20$," *Appl. Phys. Lett.* **44**(7), 651–653 (1984).
3. E. Betzig, P. L. Finn, and J. S. Weiner, "Combined shear force and near-field scanning optical microscopy," *Appl. Phys. Lett.* **60**(20), 2484–2486 (1992).
4. B. Hecht, B. Sick, U. P. Wild, V. Deckert, R. Zenobi, O. J. F. Martin, and D. W. Pohl, "Scanning near-field optical microscopy with aperture probes: Fundamentals and applications," *J. Chem. Phys.* **112**(18), 7761–7774 (2000).
5. R. Stöckle, C. Fokas, V. Deckert, R. Zenobi, B. Sick, B. Hecht, and U. P. Wild, "High-quality near-field optical probes by tube etching," *Appl. Phys. Lett.* **75**(2), 160–162 (1999).
6. S. Kawata and Y. Inouye, "Scanning probe optical microscopy using a metallic probe tip," *Ultramicroscopy* **57**(2-3), 313–317 (1995).
7. F. Zenhausern, Y. Martin, and H. K. Wickramasinghe, "Scanning Interferometric apertureless microscopy: optical imaging at 10 angstrom resolution," *Science* **269**(5227), 1083–1085 (1995).
8. R. Hillenbrand and F. Keilmann, "Material-specific mapping of metal/semiconductor/dielectric nanosystems at 10 nm resolution by backscattering near-field optical microscopy," *Appl. Phys. Lett.* **80**(1), 25–27 (2002).
9. F. M. Huang, Y. Chen, F. J. Garcia de Abajo, and N. I. Zheludev, "Optical super-resolution through super-oscillations," *J. Opt. A, Pure Appl. Opt.* **9**(9), S285–S288 (2007).
10. F. M. Huang and N. I. Zheludev, "Super-resolution without evanescent waves," *Nano Lett.* **9**(3), 1249–1254 (2009).
11. Z. Liu, H. Lee, Y. Xiong, C. Sun, and X. Zhang, "Far-Field Optical Hyperlens Magnifying Sub-Diffraction-Limited Objects," *Science* **315**(5819), 1686–1686 (2007).
12. N. Fang, H. Lee, C. Sun, and X. Zhang, "Sub-Diffraction-Limited Optical Imaging with a Silver Superlens," *Science* **308**(5721), 534–537 (2005).
13. Z. Liu, S. Durant, H. Lee, Y. Pikus, N. Fang, Y. Xiong, C. Sun, and X. Zhang, "Far-field optical superlens," *Nano Lett.* **7**(2), 403–408 (2007).
14. Z. Wang, W. Guo, L. Li, B. Luk'yanchuk, A. Khan, Z. Liu, Z. Chen, and M. Hong, "Optical virtual imaging at 50 nm lateral resolution with a white-light nanoscope," *Nat. Commun.* **2**, 218 (2011), doi:10.1038/ncomms1211.
15. J. Tominaga, T. Nakano, and N. Atoda, "An approach for recording and readout beyond the diffraction limit with an Sb thin film," *Appl. Phys. Lett.* **73**(15), 2078–2080 (1998).
16. H. Fuji, J. Tominaga, L. Men, T. Nakano, H. Katayama, and N. Atoda, "A near-field recording and readout technology using a metallic probe in an optical disk," *Jpn. J. Appl. Phys.* **39**(Part 1, No. 2B), 980–981 (2000).

17. J. Tominaga, "The application of silver oxide thin film to plasmon photonic devices," *J. Phys. Condens. Matter* **15**(25), R1101–R1122 (2003).
 18. D. P. Tsai and W. C. Lin, "Probing the near fields of the super-resolution near-field optical structure," *Appl. Phys. Lett.* **77**(10), 1413–1415 (2000).
 19. T. Shima and J. Tominaga, "Optical transmittance study of silver particles formed by AgO_x thermal decomposition," *J. Vac. Sci. Technol. A* **21**(3), 634–637 (2003).
 20. F. H. Ho, W. Y. Lin, H. H. Chang, Y. H. Lin, W. C. Liu, and D. P. Tsai, "Nonlinear optical absorption in the AgO_x-type super-resolution near-field structure," *Jpn. J. Appl. Phys.* **40**(Part 1, No. 6A), 4101–4102 (2001).
 21. F. H. Ho, H. H. Chang, Y. H. Lin, B.-M. Chen, S.-Y. Wang, and D. P. Tsai, "Functional structures of AgO_x thin film for near-field recording," *Jpn. J. Appl. Phys.* **42**(Part 1, No. 2B), 1000–1004 (2003).
 22. W.-C. Liu and C.-Y. Wen, K.-H. Chen, W. C. Lin, and D. P. Tsai, "Near-field images of the AgO_x-type super-resolution near-field structure," *Appl. Phys. Lett.* **78**, 685–687 (2001).
 23. K. P. Chiu, K. F. Lai, and D. P. Tsai, "Application of surface polariton coupling between nano recording marks to optical data storage," *Opt. Express* **16**(18), 13885–13892 (2008).
 24. D. P. Tsai and Y. H. Lin, "Near-field super-resolution optical cover glass slip or mount," U.S. Patent 6,737,167 (May 18, 2004).
-

1. Introduction

Near-field scanning optical microscopy (NSOM) is a powerful instrument for achieving ultra-high spatial resolution beyond the optical diffraction limit [1–3]. Two types of traditional NSOM exist. The first is aperture-type NSOM (a-NSOM) [4, 5] which is a coated fiber probe maintained in the near-field region of the sample surface and used for collecting near-field signals. The optical resolution of a-NSOM depends on the aperture size of the probe apex. The second NSOM is scattering-type NSOM (s-NSOM) [6–8] which is an apertureless metallic probe (or coated Si probe) apex used as a nanoscatterer to convolute the evanescent fields of the subwavelength object and transform the evanescent fields into the propagating fields. Subsequently, the subwavelength features of the object can be obtained by collecting the far-field signals. Both scanning probe microscopes can produce optical images with ultra-high spatial resolution beyond the diffraction limit. However, NSOM probes have several noticeable disadvantages, such as high cost, low throughput of light, degradation problem, and poor compatibility with various environments and samples. They seriously limited the applications of the traditional NSOM.

Recently, a number of nanophotonic applications, such as super-oscillations [9, 10] hyper lens [11], super lens [12, 13], optical virtual imaging [14], and super-resolution optical storage [15] have been proposed to overcome the optical diffraction limit. Optical sensors composed of novel materials and structures can replace NSOM probes and perform a similar function, that is, transferring (scatter) the near-field signals of the object or directly generating a hotspot to probe and interact with the object. Of these sensors, Tominaga *et al.* proposed an AgO_x-type super-resolution near-field structure for ultra-high-density optical data storage DVDs [16, 17]. Localized surface plasmons generated by photo-dissociated silver nanoparticles enhance the near-field optical signals and functions as a NSOM probe for recording and readouts [18–22]. In this study, the sandwiched AgO_x thin film is prepared on a cover glass substrate and used as a near field cover glass slip (NF-CGS). Similar to normal cover glass, this NF-CGS can be used to fix and carry various sample for traditional optical microscopy. It can achieve high spatial resolution and similar NSOM function with the advantages of a higher scanning rate, less mechanical damage, low costs, and high compatibility with conventional optical microscopy. Thus, the original disadvantages of NSOM probes are no longer a problem.

2. Experimental setup and working principle

The NF-CGS was fabricated using a reactive rf sputtering process. A normal 150- μm -thick cover glass was used as an optical transparent substrate. Multi-layered structure of ZnS-SiO₂ (130 nm)/AgO_x (15 nm)/ZnS-SiO₂ (40 nm) was deposited on the glass substrate. To prevent heat shock and oxidation of AgO_x thin film, two protective layers of ZnS-SiO₂ at 130 nm and 40 nm were prepared. The sandwiched AgO_x thin film acts as an active layer of the NF-CGS and has a refractive index about $2.8 + 0.08i$. For the sandwiched 15 nm AgO_x thin film, the average size of the photo-dissociated Ag nanoparticle is around 10 to 15 nm. The 40 nm ZnS-

SiO₂ thin film also acts as a spacer layer for precisely controlling the fixed near-field distance between the AgO_x active layer and the samples. The standard polystyrene (PS) nanospheres (Duke Scientific Corporation) 500 nm, 200 nm, and 100 nm in diameter serve as the samples and are placed on the top of the NF-CGS and pure cover glass. The solution of PS nanospheres is diluted more than 1,000 times to avoid particle aggregation. As shown in Fig. 1(a), the arrangement of PS nanospheres and substrates in our experiment was (a) 200 nm PS nanospheres and cover glass; (b) 200 nm PS nanospheres and NF-CGS; (c) a mixture of 100 nm and 500 nm PS nanospheres and cover glass; and (d) a mixture of 100 nm and 500 nm PS nanospheres and NF-CGS.

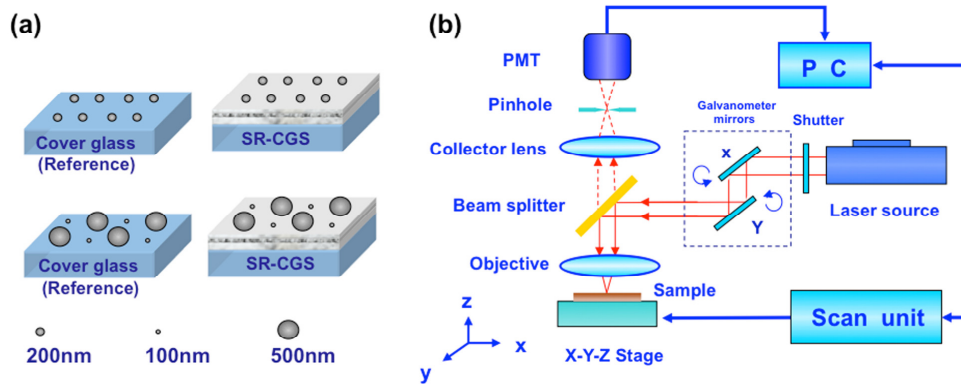


Fig. 1. (a) Various sample arrangements: 200 nm PS nanospheres and a mixture of 500 nm and 100 nm PS nanospheres placed on cover glass and NF-CGS, respectively. (b) The setup of laser scanning confocal microscopy (LCM) for the optical section of the sample.

To obtain high-resolution optical images of the sample at varied focal planes, laser-scanning confocal microscopy (Leica, ICM1000) is utilized. Figure 1(b) shows the experimental setup. The wavelength of a coherent light source is 635 nm, which correlates with the readout wavelength of super-RENS storage. High-speed imaging is achieved by high-speed scanning (4 KHz) of x-y galvanometer mirrors. Optical signals with high z-axis resolution are collected by a photomultiplier (PMT). The working principle of the NF-CGS is shown in Fig. 2. Through laser focusing, a small region of the AgO_x active layer is heated above the threshold temperature, decomposing into silver nanoparticles and oxygen. The photo-dissociated silver nanoparticles act as a scattering center for activating the near-field optical imaging process. They can enhance the evanescent waves and perform the function of a near-field apertureless probe, that is, transform the evanescent waves into the propagating waves. The coupling and enhancing effects [23] between the photo-dissociated silver nanoparticles and the subwavelength features of the sample in near-field region play an important role here. Subsequently, the subwavelength features of the samples can be obtained in the far-field signals, and the sub-diffraction-limited images can be reconstructed. Furthermore, the decomposed oxygen is well confined in the local region because of the sandwiched structure. This means that when the laser power is removed, the silver nanoparticles and oxygen can be recombined to form AgO_x again. Thus, NF-CGS can be employed as a flat substrate for near-field optical imaging because of the advantageous reversible AgO_x layer. However, a focused laser beam with suitable laser scanning optical microscopy power is required. The irreversible damage of the NF-CGS that results from excessively intense incident light beams is shown in the picture embedded in the bottom right of Fig. 2.

We performed the optical section imaging of the nanospheres using an oil immersion objective lens (100x, 1.25) with a laser scanning confocal microscope. A reflective optical image was taken every 6 nm along the z-axis of the substrate. The effect of using NF-CGS

was compared with that of the cover glass according to the resolving of nanospheres at varied focal planes. To identify the focused position of the laser on the sample, the intensity of the background light from the measured images were averaged and the reflected z-scan spectrum was plotted, as shown in Fig. 3. Figure 3(a) shows the spectrum of the cover glass, and Fig. 3(b) shows that of the NF-CGS. The results indicate that using NF-CGS has a higher relative reflectance and is obviously varied in the distribution of spectral lines with the cover glass. In order to confirm the reproducibility of the experiments, the measuring position was altered and the new spectrum was plotted accordingly (CMYK curve). The slightly discontinuity and shifting in these curves may be caused by imprecise mechanical and optical microscope components. The focused laser plane position on each optical image can be estimated according to the intensity changes of the curves. To conduct analysis, hundreds of optical images were observed and the focal planes of the representative images for the cover glass and the NF-CGS were marked as f1, f2, f3, and F1, F2, F3, F4, F5.

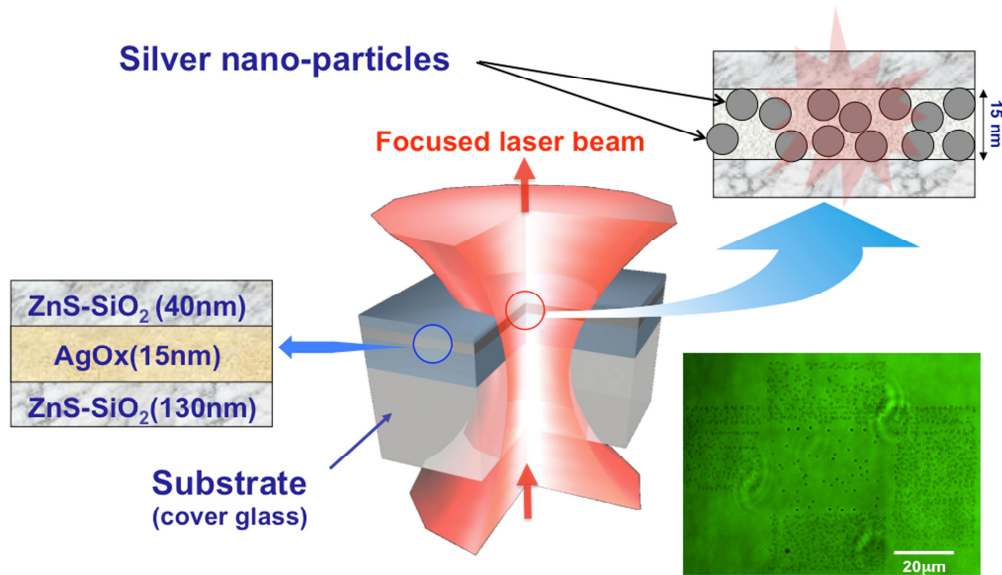


Fig. 2. The working principle of the NF-CGS: The photo-dissociated silver nanoparticles enhance the evanescent waves and perform the function of a near-field apertureless probe to transform the evanescent waves into the propagating waves. The subwavelength information of the nanospheres can be subsequently obtained. The near-field distance between the active layer (AgO_x) and the sample (PS nanospheres) is precisely controlled by a ZnS-SiO₂ (40 nm) spacer layer. The picture embedded in the bottom right shows the irreversible NF-CGS damage caused by inappropriate laser power.

3. Results and discussion

As shown in Fig. 3(a), the z-scan spectrum curve of the cover glass substrate is relatively smooth. The position of f1 shows that the focal plane of the laser is still within the glass, whereas the position of f3 indicates that the focal plane is in the air and far from the sample. The position of f2 is at the peak of the curve, which means that the focal plane of the laser is at the interface of the glass and air. In Fig. 4, the columns represent the focal planes (f1, f2, and f3) and the rows represent the images of the 200 nm, 500 nm, and 100 nm nanosphere samples, with corresponding cross-sectional images on the right side, and where the scale of the blue bar is 0.2 μm. In the f1 focal plane, the optical images of the three sizes of nanospheres appeared defocused; however, the background light was sustained by the partial reflection of the interface between the glass and air. In the f2 focal plane, the nanospheres

with a diameter of 200 nm and 100 nm were completely covered by the depth of focus (DOF) of laser. Because the scale is less than the diffraction limit, the nanospheres cannot be resolved, as shown in the cross-sectional images. For the nanospheres with a diameter of 500 nm, part of the structure that is covered by the DOF of laser can be successfully resolved because of its larger size. The illuminated light is scattered by the nanospheres and lead to the wide dip in the cross-sectional images. A reflected signal at the center of the nanospheres responds to material dielectric contrast and the FWHM of the intensity profile represents the resolution in the system. The f3 focal plane is located in the air region away from the nanospheres with a diameter of 200 nm and 100 nm. In these two samples, no image is displayed because no background light is reflected by the interface; however, nanospheres with a diameter of 500 nm fall within the DOF; thus, they can be clearly resolved.

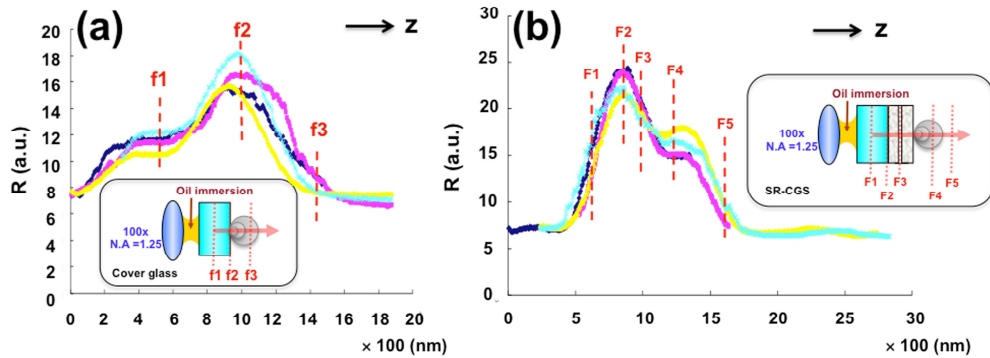


Fig. 3. The reflected z-scan spectrum of (a) the cover glass and (b) the NF-CGS.

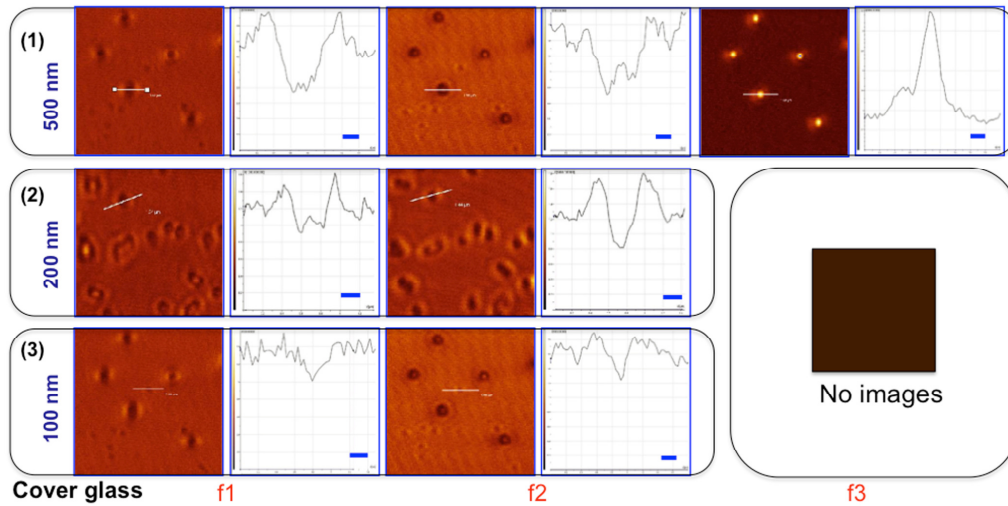


Fig. 4. Optical and cross-sectional images of three sizes of nanospheres with varied focal planes (f1, f2, f3, as shown in Fig. 3(a)), using a cover glass substrate.

As shown in Fig. 3(b), the z-scan spectrum curve of NF-CGS substrate has a higher reflectance and differs from that of the cover glass. F1 shows that the focal plane of laser falls within the glass. F2 shows that the laser focal plane falls near the interface between the glass and the sandwiched AgO_x thin film. The laser in F3 falls at the position from where F2 is forward shifted by 130 nm, which is approximately where the laser focal plane falls within the AgO_x active layer. F4 shows that the focal plane of laser is away from the sandwiched

AgO_x thin film and falls within the nanospheres. F5 shows that the laser focal plane is partly in the air away from the sample. In Fig. 5, the columns represent the focal planes (F1, F2, F4, and F5), and the rows sequentially correspond to the nanospheres with diameters of 200 nm, 500 nm, and 100 nm. The optical image of the F3 focal plane (the laser focusing position on the AgO_x layer) is shown in Fig. 6 to enable further discussion. In the F1 focal plane, all three nanospheres sizes appear defocused. Regarding the F2 focal plane, although nanospheres with a diameter of 100 nm cannot be resolved, nanospheres with a diameter of 200 nm have the preset features of being resolvable (in a cross-sectional diagram). Additionally, nanospheres with a diameter of 500 nm can be observed because of their larger size. The focal planes of F4 fall away from the nanospheres with diameter of 100 nm and 200 nm and enter the air region, or they fall in the nanospheres with a diameter of 500 nm. Thus, nanospheres with a diameter of 100 nm or 200 nm cannot be resolved, whereas nanospheres with a diameter of 500 nm can be resolved. The F5 focal plane is located in the air region away from the nanospheres. Only nanospheres with a diameter of 500 nm can be clearly resolved because they fall within the DOF. Significantly, the laser intensity used to measure nanospheres with a diameter of 200 nm and 500 nm plus 100 nm differed slightly, varying the image background brightness.

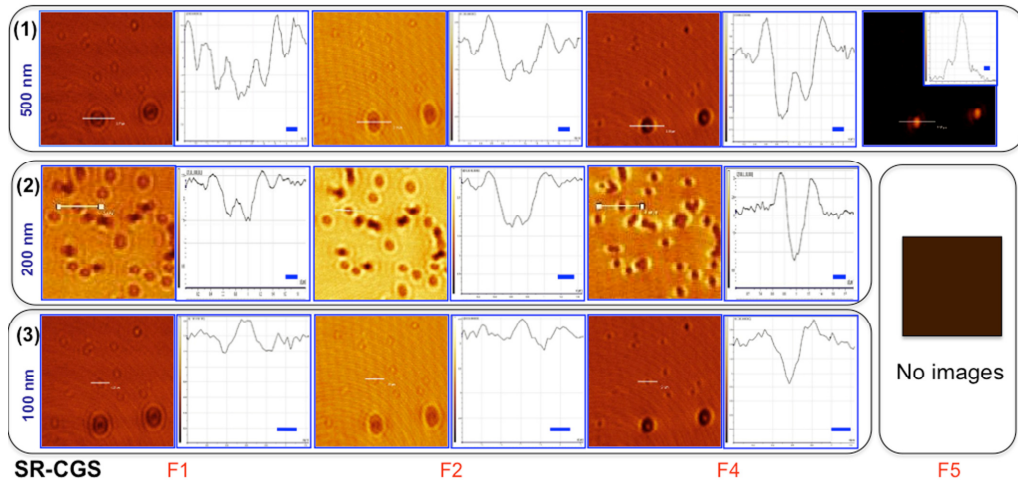


Fig. 5. Optical and cross-sectional images of three sizes of nanospheres with varied focal planes (F1, F2, F4, F5, as shown in Fig. 3(b)), using a NF-CGS substrate.

When the laser is focusing on the AgO_x layer of the NF-CGS (F3 focal plane), in addition to nanospheres 500 nm in diameter, nanospheres both 200 nm and 100 nm in diameter can be observed, as shown in Fig. 6(a). However, the sizes of the nanospheres in the optical cross-sectional images do not correspond exactly to the original scale; instead, the sizes were measured as approximately 300 nm, 173 nm, and 100 nm. This is because the localized surface plasmon excited by photo-dissociated silver nanoparticles is only effective in the near-field region; therefore, only the bottom of the nanospheres can be successfully resolved. As shown in Fig. 6(b), a comparison of the geometric relationship among the nanospheres also indicates that the effective range of the NF-CGS in z-axis is nearly 50 nm, as marked by the red dashed line. The experimental results support the working principle of NF-CGS and its applicability.

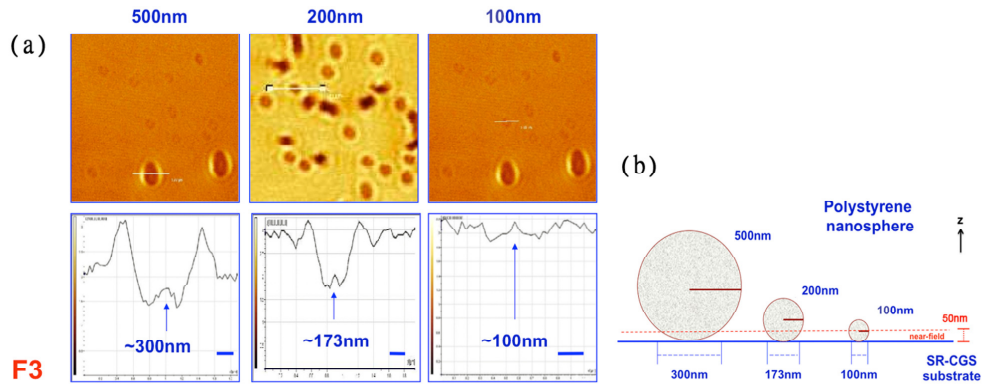


Fig. 6. (a) Optical and cross-sectional images of the three nanospheres sizes with the F3 focal plane (laser focusing on the AgO_x active layer), using a NF-CGS substrate. (b) The geometric relationship among the nanospheres. The region below the red dashed line shows the effective range of the NF-CGS.

4. Conclusion

This study successfully developed a simple, low-cost, and novel cover glass slip, NF-CGS, which is suitable for different samples and various environments, compatible with traditional optical microscopy for a high scanning speed, and provides ultra-high near-field optical resolution beyond the diffraction limit. During the experiments, a laser-scanning confocal microscope was used to obtain cross-sectional images of the nanospheres, in three sizes, on the cover glass and NF-CGS substrate at various focal planes. The results show that the polystyrene nanospheres 200 nm and 100 nm in diameter can only be resolved on the NF-CGS substrate and when the laser is focused accurately on the AgO_x active layer. This indicates that the photo-dissociated silver particles in the AgO_x active layer act as a scattering center for activating the near-field optical imaging process. This study developed a novel solution for nano-optical inspections and related applications. The results of this study have been granted a U.S. patent [24].

Acknowledgments

The authors thank financial aids from National Science Council, Taiwan under grant numbers 99-2911-I-002-127, 99-2120-M-002-012, 100-2923-M-002-007-MY3 and 100-2120-M-002-008. Authors are grateful to the Molecular Imaging Center of NTU and Research Center for Applied Sciences, Academia Sinica, Taiwan for their support.